



Cite this: *Environ. Sci.: Water Res. Technol.*, 2023, 9, 772

## Functionalised polymeric materials for the removal of arsenate from contaminated water†

Anna Segues Codina,<sup>a</sup> Aaron Torres Huerta,<sup>a</sup> Hany Fathy Heiba,<sup>b,c</sup> Jay C. Bullen,<sup>b</sup> Dominik J. Weiss<sup>\*b</sup> and Ramon Vilar<sup>id\*<sup>a</sup></sup>

Inorganic arsenic is a carcinogen and, in some regions, one of the biggest contaminants in drinking water. The World Health Organisation (WHO) has indicated that over 140 million people worldwide are drinking water with levels of arsenic above the recommended guideline value of 10  $\mu\text{g L}^{-1}$ . Therefore, there is a pressing need to find low-cost technologies for the removal of inorganic arsenic from water. As part of our efforts to tackle this problem, we previously developed an efficient sorbent material (ImpAs) based on a polymeric support (HypoGel) functionalised with a selective chemical receptor for arsenate (*i.e.* arsenic(v)). With the aim to lower the production cost of this material and improve its arsenate removal capacity, we have studied other polymeric materials as solid supports. Herein, we report the synthesis of new inexpensive sorbent materials by covalently attaching our previously reported arsenate receptor onto Merrifield and Purolite C106 polymer beads. We carried out batch and flow-through experiments with the new polymeric materials demonstrating that they have up to 60% higher arsenate removal capacities than the original functionalised HypoGel material. Furthermore, the new polymeric materials operate very well under flow-through conditions, removing over 99% of arsenate present in solutions containing low (15  $\mu\text{g L}^{-1}$ ) and high (300  $\mu\text{g L}^{-1}$ ) levels of arsenate. We also report on the lower production cost of the new Purolite-based material as compared to the original functionalised HypoGel polymer beads.

Received 2nd December 2022,  
Accepted 16th January 2023

DOI: 10.1039/d2ew00917j

rsc.li/es-water

### Water impact

It is estimated that over 226 million people are exposed to concentrations of arsenic in drinking water above the WHO guideline value of 10  $\mu\text{g L}^{-1}$  (which is deemed provisional due to current limitations in removal and detection methods). Herein we report new low-cost materials that remove over 99% of arsenate from water reducing its concentration to below 3  $\mu\text{g L}^{-1}$ .

## 1. Introduction

The presence of arsenic in water is a major environmental challenge worldwide. Recent studies estimate that more than 226 million people are exposed to concentrations of arsenic in drinking water above the guideline value of 10  $\mu\text{g L}^{-1}$ , established by the World Health Organisation (WHO) in 1993.<sup>1</sup> This is a particularly acute problem in Bangladesh, India, China and Pakistan, with the situation in Bangladesh being described by the WHO as the “largest mass poisoning of a population in history”.<sup>2</sup> While most high-income countries use the WHO 10  $\mu\text{g L}^{-1}$  guideline value, this is

deemed “provisional” since risk assessment data indicate that a lower value would be more appropriate. Consequently, due to health and environmental concerns, some governments have put in place more stringent legislation regarding the allowed levels of arsenic in water (*e.g.* in Denmark, the officially recommended maximum level of arsenic in water is 5  $\mu\text{g L}^{-1}$ ).<sup>1</sup> Therefore, there is a pressing need to improve low-cost technologies that are effective at removing arsenic from water.

Arsenic is found naturally in a large number of minerals and is released into water by dissolution. Human activity is another source of contamination, mainly caused by industrial processes, mining activity, use of pesticides and fossil fuel combustion.<sup>3</sup> In most natural waters, the prevalent forms of arsenic are arsenate (a tetrahedral As(v) oxyanion which at pH between 6 and 8 is partially protonated:  $\text{H}_2\text{AsO}_4^-$  and  $\text{HAsO}_4^{2-}$ ) and arsenite (a trigonal planar As(III) compound which is fully protonated except at very high pH values). Arsenate dominates in oxygen rich waters, whereas arsenite

<sup>a</sup> Department of Chemistry, Imperial College London, White City Campus, 82 Wood Lane, London W12 0BZ, UK. E-mail: r.vilar@imperial.ac.uk

<sup>b</sup> Department of Earth Science and Engineering, Imperial College London, South Kensington, London SW7 2AZ, UK. E-mail: d.weiss@imperial.ac.uk

<sup>c</sup> National Institute of Oceanography and Fisheries (NIOF), Cairo, Egypt

† Electronic supplementary information (ESI) available. See DOI: <https://doi.org/10.1039/d2ew00917j>



is the prevalent form under anaerobic conditions. Due to the lack of electrostatic charge, it is generally more difficult to remove arsenite than arsenate from contaminated water. Therefore, waters containing As(III) species are generally treated with oxidizing agents to convert them to As(V).<sup>4</sup>

While natural levels of arsenic in water are typically between 1 to 10  $\mu\text{g L}^{-1}$ , in the most affected areas concentrations can reach more than 100  $\mu\text{g L}^{-1}$ .<sup>3</sup> The prolonged exposure of humans to these high levels of arsenic causes cancer and skin lesions and has been associated with diabetes and cardiovascular diseases.<sup>5</sup> Therefore, it is essential that water for human consumption is pre-treated to remove arsenic.

Arsenic remediation approaches include membrane separation, precipitation, coagulation, adsorption and ion exchange processes.<sup>6</sup> The last two are routinely used since they are generally low-cost, easy to operate and produce minimal waste. For example, metal oxides (such as iron and aluminium oxides) are widely used adsorbing materials for arsenic removal.<sup>7–9</sup> Ion-exchange resins have also shown to be effective in the removal of arsenic from water<sup>10,11</sup> and, when considering life-cycle analysis, more sustainable than adsorbing materials based on metal oxides.<sup>12</sup> The effectiveness of the adsorption/ion-exchange processes is sensitive to several factors such as fouling of the adsorbent

material, pH of water, flow rate and arsenic oxidation state. Furthermore, most materials quickly saturate especially due to non-selective adsorption of more abundant competitor ions, including sulphate and carbonate.

We previously developed a functionalised polymeric material (**ImpAs-HypoGel**) based on a di-zinc(II) receptor attached to commercially available polystyrene HypoGel beads.<sup>13</sup> This receptor, binds selectively to arsenate *via* coordination of its oxygen atoms to the zinc(II) metal centres (Fig. 1). Thus, unlike ‘traditional’ ion-exchange resins, **ImpAs-HypoGel** does not operate *via* simple electrostatic interactions, but it is tailored to bind selectively to arsenate. While many chemical receptors have been reported for a range of oxyanions (such as phosphate,<sup>14</sup> sulphate<sup>15</sup> and nitrate<sup>16</sup>), there are very few examples that bind to arsenate.<sup>17–19</sup> In our previous study,<sup>13</sup> we showed that **ImpAs-HypoGel** adsorbs arsenate with very high capacity and good selectivity over other anions such as sulphate and nitrate. In addition, it can be regenerated and reused easily without loss of performance even after several cycles. These properties allowed us to successfully use **ImpAs-HypoGel** to remove arsenate from drinking water both in batch treatments and in flow applications. In further studies, we also demonstrated that this material can be used for the determination of arsenic speciation (*i.e.* separation of arsenic(V) and

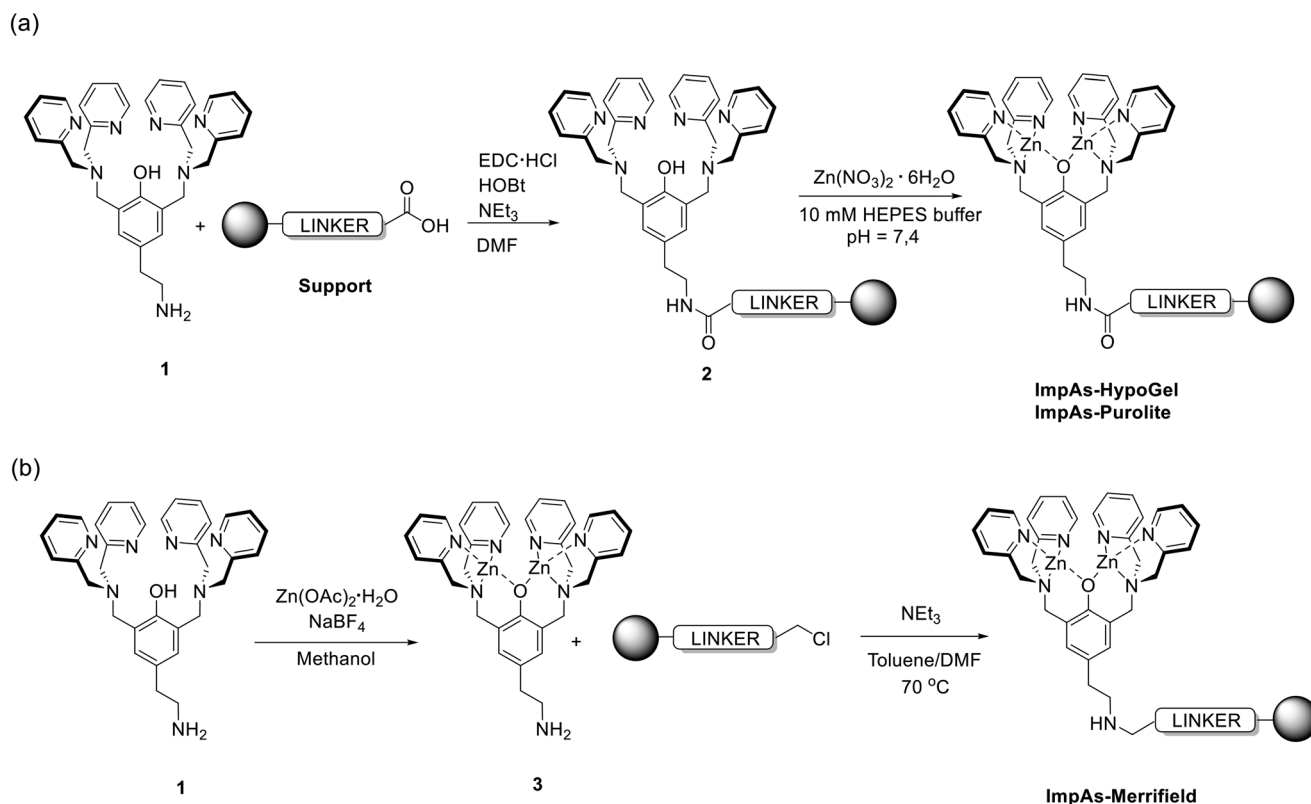


**Fig. 1** General reaction scheme for the synthesis of functionalised polymeric materials. (a) Synthesis of **ImpAs-HypoGel** (our previous work<sup>13</sup>) and **ImpAs-Purolite** *via* attachment of ligand **1** to polymers followed by coordination of zinc(II) to yield the arsenate receptors on the beads. (b) Synthesis of **ImpAs-Merrifield** *via* direct attachment of zinc(II)-based receptor to the Merrifield polymer. Anions have been omitted for clarity (in all cases, the di-zinc receptor has an overall charge of 3+ and hence three monovalent counter-anions are associated to the receptor).



arsenic(III) in the field and laboratory.<sup>20</sup> This can be achieved since **ImpAs-HypoGel** binds arsenate but not arsenite which, combined with techniques to determine total arsenic such as UV/vis or ICP-MS, allowed us to determine the concentration of both arsenate and arsenite in groundwater.

**ImpAs-HypoGel** has very good arsenate-adsorbing properties but is expensive to produce (as compared to 'traditional' ion-exchange resins and arsenic removing materials based on metal oxides), and its sorption capacity is not yet optimised (*i.e.* more receptor could be loaded per unit mass of polymer). To improve these features, herein we report the development of two new adsorbing materials where the arsenic-binding di-zinc(II) receptor we previously developed (compound **3** in Fig. 1), has been attached to two different polymeric supports, Purolite C106 and Merrifield beads. The former is a polyacrylic microporous polymer while the latter is a divinylbenzene cross-linked polystyrene material. These polymeric solid supports were selected due to: (i) their commercial availability and lower price compared to HypoGel (particularly Purolite C106); (ii) to allow testing the effect of different bead sizes (ranging from 40 to 1600  $\mu\text{m}$ ) on the performance of the adsorbing materials; (iii) the possibility of increasing the density of active sites on the polymer beads (and therefore the capacity for arsenate removal of the final materials).

## 2. Materials and methods

### 2.1 Materials

HypoGel 200 CHO was purchased from Rapp Polymere, Purolite C106 from Purolite and Merrifield resin (200–400 mesh) from Sigma Aldrich (see Table 1 for key parameters for the three polymers used in this work). Compound **1** (Fig. 1) was prepared following our previously reported synthetic procedure.<sup>13</sup>

### 2.2 Synthesis of ImpAs-HypoGel

This was carried out by small modifications to our previously reported procedure.<sup>13</sup>

Step 1 – coupling compound **1** to HypoGel beads: a plastic bottle was loaded with compound **1** (3.99 g, 7.12 mmol), HypoGel polymer beads (4.81 g, 3.56 mmol), EDC-HCl (0.82 g, 4.27 mmol), HOBt (0.58 g, 4.27 mmol) and triethylamine (1.24 ml, 8.90 mmol). DMF (50 mL) was added as a solvent. This mixture was mechanically shaken for 48 hours at room temperature after which time it was filtered and the resulting solid was washed with DMF, methanol, dichloromethane and diethyl ether. The isolated solid was subsequently dried under vacuum until the weight was constant.

Step 2 – loading zinc(II) to functionalised HypoGel beads: a plastic bottle was loaded with  $\text{Zn}(\text{NO}_3)_2 \cdot 6\text{H}_2\text{O}$  (4.19 g, 14.07 mmol), the HypoGel beads functionalised with compound **1** (6.78 g, 0.52 mmol  $\text{g}^{-1}$ ) prepared in step 1, and 40 mL of HEPES buffer (10 mM, pH 7.4). The mixture was mechanically shaken for 48 hours, then the resulting suspension was filtered, and the obtained solid was washed three times with 20 mL of HEPES buffer. The isolated solid was subsequently dried under vacuum until the weight was constant (7.02 g of **ImpAs-HypoGel**). The remaining filtrate plus the HEPES buffer used for the washings were kept to determine the concentration of unreacted zinc(II) by UV/vis spectroscopy (see below).

### 2.3 Synthesis of ImpAs-Purolite

Step 1 – coupling compound **1** to Purolite C106 beads: a plastic bottle was loaded with compound **1** (4.51 g, 8.06 mmol), Purolite C106 (1.15 g, 4.03 mmol), EDC-HCl (0.92 g, 4.83 mmol), HOBt (0.65 g, 4.83 mmol) and triethylamine (1.4 ml, 10.07 mmol). DMF (50 mL) was added as a solvent. This mixture was mechanically shaken for 48 hours at room temperature after which time it was filtered and the resulting solid was washed with DMF, methanol, dichloromethane and diethyl ether. The isolated solid was subsequently dried under vacuum until the weight was constant.

Step 2 – loading zinc(II) to functionalised Purolite C106 beads: a plastic bottle was loaded with  $\text{Zn}(\text{NO}_3)_2 \cdot 6\text{H}_2\text{O}$  (2.34 g, 7.86 mmol), Purolite functionalised with compound **1** (2.25 g, 0.68 mmol  $\text{g}^{-1}$ ) prepared in step 1, and 40 mL of HEPES buffer (10 mM, pH 7.4). The resulting mixture was mechanically shaken for 48 hours. The resulting suspension was filtered, and the corresponding solid obtained was washed three times with 20 mL of HEPES buffer. The isolated solid was subsequently dried under vacuum until the weight was constant (2.92 g of **ImpAs-Purolite**). The remaining filtrate plus the HEPES buffer used for the washings were kept to determine the concentration of unreacted zinc(II) by UV/vis spectroscopy (see below).

### 2.4 Synthesis of ImpAs-Merrifield

Step 1 – synthesis of receptor **3**: a mixture of compound **1** (0.397 g, 0.71 mmol) and  $\text{Zn}(\text{OAc})_2 \cdot 2\text{H}_2\text{O}$  (0.312 g, 1.42 mmol) in methanol (30 ml) was stirred for 2 hours at room temperature. Then,  $\text{NaBF}_4$  (0.078 g, 0.71 mmol) was added, and the reaction mixture was stirred overnight. After this time, all volatiles were removed under reduced pressure. The remaining solid was washed three times with ethyl acetate and used for the next step without further purification.

**Table 1** Characteristics of solid supports used in this study as reported by the commercial suppliers<sup>21–23</sup>

Support	Size of particle ( $\mu\text{m}$ )	BET surface area ( $\text{m}^2 \text{g}^{-1}$ )	Pore volume ( $\text{cm}^3 \text{g}^{-1}$ )	Functionalisation	Capacity ( $\text{mmol g}^{-1}$ )	Price (£ per g)
HypoGel	110–150	1.17	0.0003	COOH	0.74	20
Purolite C106	300–1600	1.61	0.0019	COOH	3.5	0.007
Merrifield	37–74	—	—	Cl	3.9	2.03



Step 2 – coupling of receptor 3 to polymer Merrifield beads: the di-zinc(II) complex was attached to the Merrifield resin by mixing a DMF (4 mL) solution containing compound 3 (0.4 g, 0.58 mmol) and triethylamine (0.7 mL, 5.04 mmol), with a toluene (8 mL) suspension of the Merrifield resin (0.1 g, 0.39 mmol). This mixture was stirred for 24 hours at 70 °C after which time the resulting solid was separated by centrifugation and washed with toluene, DMF, methanol, water and acetone. The remaining filtrate plus the toluene and DMF used for the washings were kept in order to determine the concentration of unreacted compound 3 by UV/vis spectroscopy (see below). The isolated solid was subsequently dried under a flow of nitrogen until the weight was constant (0.12 g of **ImpAs-Merrifield**).

### 2.5 Determination of receptor loading onto HypoGel and Purolite C106

The amount of receptor attached to **ImpAs-HypoGel** and **ImpAs-Purolite** was indirectly determined by quantifying unreacted zinc(II) left in solution after the attachment reaction (see above). The metal ion concentration was determined *via* UV/vis spectroscopy using pyrocatechol violet (PV) a colorimetric indicator that changes colour upon interaction with zinc(II). Firstly, a calibration curve was obtained by adding increasing amounts of zinc(II) (aliquots of a 13.5 mM Zn(NO<sub>3</sub>)<sub>2</sub> standard solution) to PV (700 µL from a 100 µM stock solution) in the measuring cuvette. The absorbance after each addition was measured at 605 nm and it was plotted against the concentration (see Fig. S1† for calibration curve). Having established the calibration curve, samples were measured by adding an aliquot of the corresponding sample to 700 µL of 100 µM solution of PV in a UV/vis cuvette. The absorbance at 605 nm was measured and this was used to determine the concentration of unreacted zinc(II) which allowed us to determine the amount of coordinated zinc(II) and hence the loading of the receptor onto the corresponding solid support.

### 2.6 Determination of the receptor loading onto ImpAs-Merrifield

The amount of receptor loaded onto **ImpAs-Merrifield** was indirectly determined by quantifying the amount of unreacted compound 3 (Fig. 1) left in solution after the attachment reaction (see above). The concentration of this compound was determined *via* UV/vis spectroscopy using PV in an analogous fashion to the determination of free zinc(II) (see previous section); for the calibrations curve, a 13.5 mM solution of compound 3 was used (see Fig. S2†). It should be noted that in this method it is not free zinc(II) ions that are detected but the intact metal complex. This is based on the ability of PV to bind to the two empty coordination sites on the zinc(II) complex as has been previously documented.<sup>24,25</sup>

### 2.7 Scanning Electron Microscopy (SEM) of polymer beads

The polymer samples were loaded onto a sample holder then coated with gold and finally scanned using high resolution

SEM Zeiss Gemini Sigma300 operating at either 5 kV or 10 kV (see Fig. 3), supplied with a High Definition Backscatter Detector (HD BSD).

### 2.8 Determination of the arsenic adsorption isotherms using batch reactions

An arsenate stock solution (1000 mg L<sup>-1</sup>) was prepared by dissolving Na<sub>2</sub>HAsO<sub>4</sub>·7H<sub>2</sub>O (0.416 g, 1.33 mmol) in 100 mL of MilliQ water; pH was adjusted to 7.4 by adding a few µL of 1 M HCl. To build the adsorption isotherms, several arsenate solutions – in a range of concentrations from 3 mg L<sup>-1</sup> to 50 mg L<sup>-1</sup> – were prepared by diluting the stock solution with HEPES buffer (10 mM, pH 7.4). 10 mL aliquots of each solution were placed in a 15 mL Falcon tube and 5 mg of sorbent was added to each tube. The different mixtures were shaken at 135 rpm for 24 hours at room temperature. After this time, the sorbent of each suspension was removed by centrifugation. The concentration of arsenate that remained in the solution was determined by inductively coupled plasma mass spectrometry (ICP-MS).

### 2.9 Protocol to determine arsenate removal in flow conditions

One gram of the corresponding sorbent (*i.e.* **ImpAs-HypoGel**, **ImpAs-Purolite** or **ImpAs-Merrifield**) was placed in a 10 mL polypropylene column between two filters, to prevent leaching of the solid (see Fig. 2), to determine the arsenate removal from water in a flow-through configuration. The sorbent was cleaned several times with HEPES buffer and stored with this solution to ensure good performance. Solutions of 15 µg L<sup>-1</sup> and 300 µg L<sup>-1</sup> of arsenate in HEPES buffer (10 mM, pH 7.4) were prepared from a 1000 mg L<sup>-1</sup> stock solution. 50 mL of each solution were passed through each column using a peristaltic pump. The experiment was performed at two different flow rates – 1 mL min<sup>-1</sup> and 5 mL min<sup>-1</sup> – for each solution and sorbent. The solution was

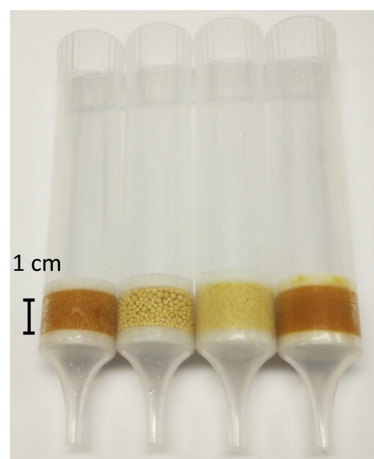


Fig. 2 Columns used in the flow through experiments with 1 g of sorbent (from left to right: **ImpAs-HypoGel**, **ImpAs-Purolite**, ground **ImpAs-Purolite** and **ImpAs-Merrifield**). The bed length was 1 cm for **ImpAs-Purolite**, and 0.9 cm in for the other sorbents.



collected after passing through the column and the arsenate content in this effluent was analysed by ICP-MS.

### 2.10 Determination of arsenic by ICP-MS

All the samples were acidified with HNO<sub>3</sub> 2% (v/v) and analysed with an Agilent 7900 quadrupole ICP-MS. External calibration curves with 6 standards were constructed using an arsenate multi-element standard. The detection limit for arsenate at ICP-MS was 0.0971 µg L<sup>-1</sup>.

## 3. Results and discussion

### 3.1 Synthesis and characterisation of ImpAs with different solid supports

The polymers functionalised with the arsenate receptor were synthesised as shown in Fig. 1. For **ImpAs-Purolite**, we followed an analogous procedure to the one we previously reported for the HypoGel equivalent.<sup>13</sup> Compound **1** was attached to Purolite C106 and subsequently loaded with zinc(II) to generate the receptor on the beads. This procedure was slightly modified for the synthesis of **ImpAs-Merrifield**

since the protocol used above did not give good quality adsorbing material. To this end, compound **1** was first reacted with Zn(OAc)<sub>2</sub> to yield the active metallo-receptor **3** and subsequently reacted with the Merrifield resin as shown in Fig. 1.

Each polymer starting material has a different number of active sites per unit mass of polymer for functionalisation (see Table 1) with Purolite C106 displaying five times more reactive carboxylic acid groups – *i.e.* the functional group used to attach the arsenate receptor onto the beads – than HypoGel. Based on the number of reactive sites reported by the polymers' suppliers, we determined the loading of the arsenate receptor onto each polymer. To do this, we quantified the amount of zinc(II) in the case of **ImpAs-HypoGel** and **ImpAs-Purolite**, and compound **3** in the case of **ImpAs-Merrifield**, left in solution after reacting with the corresponding polymer. The quantification was achieved by UV/vis spectroscopy using pyrocatechol violet (PV), a well-established dye to determine the concentration of metal ions including zinc(II) and its complexes in solution (see ESI† for calibration curves and details). The functionalised polymers

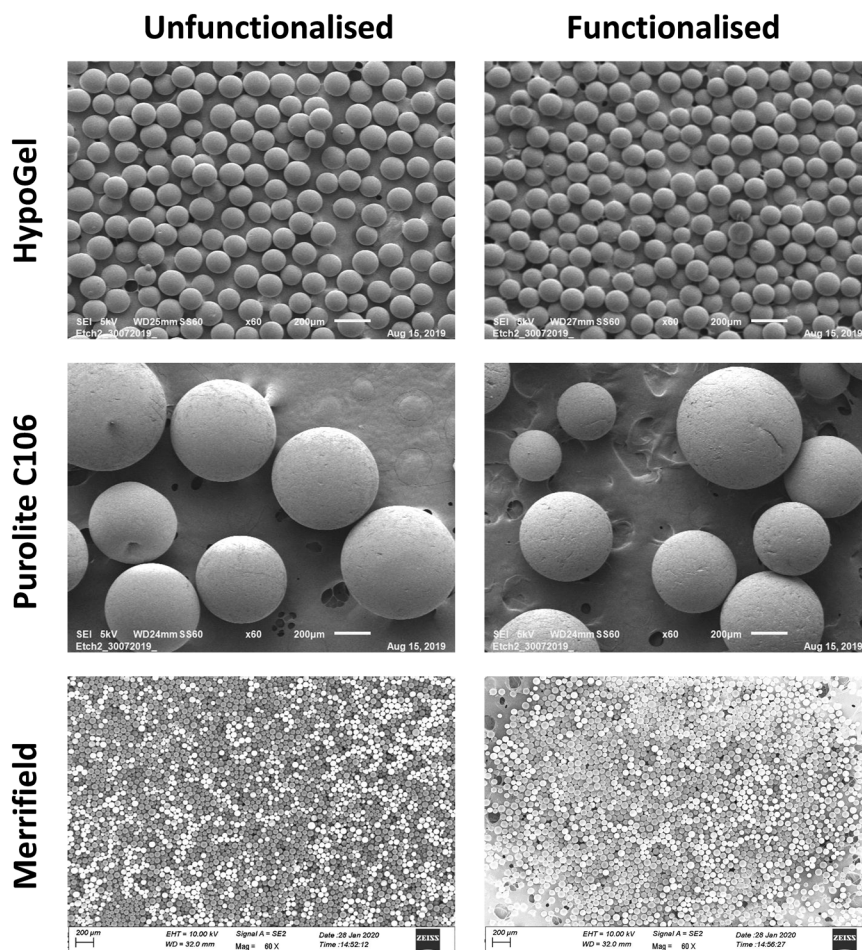


**Fig. 3** SEM images of the unfunctionalized (left) and functionalised polymer beads (right) with **ImpAs-HypoGel** (top), **ImpAs-Purolite** (middle) and **ImpAs-Merrifield** (bottom). The scale bars (200 µm) are shown in each pair of images and the magnification (60×) is the same for the three sets of images to allow comparison of the particle size of each polymer bead. Images were recorded using a SEM Zeiss Gemini Sigma300 instrument operating at either 5 kV (top two rows) or 10 kV (bottom row).



were thoroughly washed prior to quantification to ensure that all physisorbed zinc(II) or compound **3** were removed from the beads. Loading of the two new polymers was higher than that of **ImpAs-HypoGel**, particularly with Purolite C106 (see Table 2). This is an important improvement since it increases the sorbent capacity to remove arsenate from water.

Following the quantification of receptor loading on the three polymeric materials, it was of interest to establish whether the morphology of the beads changed upon functionalisation using Scanning Electron Microscopy (SEM). We found that the spherical morphology and integrity of the beads did not change significantly by the addition of the arsenate receptor (Fig. 3). The **ImpAs-HypoGel** beads have diameters ranging between *ca.* 108 to 150  $\mu\text{m}$  (which is practically the same than the size range provided by the suppliers of the unmodified HypoGel beads). The particles of **ImpAs-Purolite**, have diameters ranging from *ca.* 480 to 660  $\mu\text{m}$ , which is within the same range than the unfunctionalised Purolite C106 beads (between 300 to 680  $\mu\text{m}$ ). The **ImpAs-Merrifield** beads have diameters ranging between 40 and 75  $\mu\text{m}$ , (which is in the size range provided by the suppliers of the unmodified Merrifield beads).

### 3.2 Arsenate adsorption capacities through batch experiments

The arsenate adsorption capacities of the three sorbent materials were determined by incubating the corresponding material with aqueous solutions of  $\text{Na}_2\text{HAsO}_4\cdot\text{H}_2\text{O}$  at concentrations ranging between 3  $\text{mg L}^{-1}$  and 50  $\text{mg L}^{-1}$ . The experimental data was fitted to the Langmuir isotherm equation:

$$Q_e = \frac{b \cdot Q_{\text{max}} \cdot C_e}{1 + b \cdot C_e} \quad (1)$$

where,  $Q_e$  corresponds to the amount of arsenate adsorbed in equilibrium ( $\text{mg g}^{-1}$ ),  $b$  is an affinity coefficient ( $\text{L mg}^{-1}$ ),  $Q_{\text{max}}$  is the calculated maximum adsorption capacity ( $\text{mg g}^{-1}$ ) and  $C_e$  the concentration of arsenate in solution at equilibrium ( $\text{mg L}^{-1}$ ) (which was calculated by subtracting the concentration of As(v) remaining in solution after batch reaction, from the concentration of As(v) added to the test tube).

The isotherms are shown in Fig. 4 and the adsorption capacities were determined using the Langmuir model (see Table 3). Since arsenate binds to the functionalised receptors, its removal is through monolayer adsorption, and therefore the Langmuir adsorption isotherm is the most appropriate adsorption isotherm model. Furthermore, the adsorption

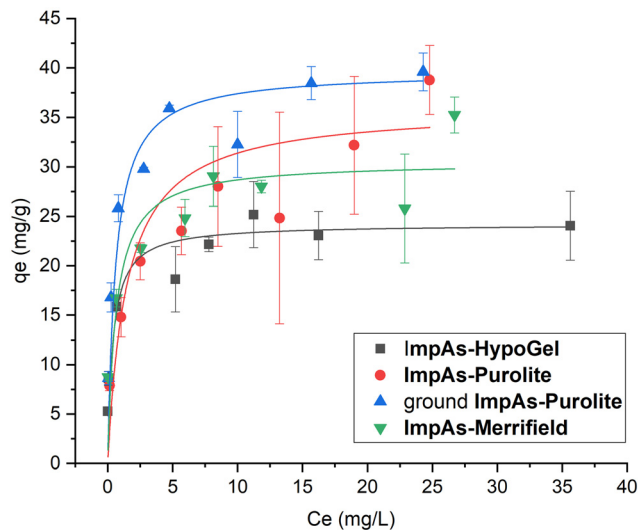


Fig. 4 Arsenate adsorption isotherms of the sorbents performed with solutions between 3  $\text{mg L}^{-1}$  and 50  $\text{mg L}^{-1}$  of arsenate in HEPES buffer (10 mM, pH 7.4) for 24 hours at room temperature. The measurements were performed in triplicate (see ESI† for all the data).

isotherms reach a plateau confirming the Langmuir monolayer adsorption mechanism.

The material with the highest arsenate capacity is **ImpAs-Purolite** ( $36 \pm 13 \text{ mg g}^{-1}$ ). However, as can be seen from the error bars of the data points at different concentrations, there was significant variation between measurements. We attribute this to higher errors when weighing out the material due to the larger size of the beads as compared to the other polymers as well as some of the beads adhering to the weighing vessel. To address this, the **ImpAs-Purolite** beads were physically ground (using mortar and pestle) to a powdery material which was easier to weigh out accurately and pack in short columns (see below for discussion of the flow through experiments). Fig. 4 and Table 3, show that there was very little variability in repeat measurements using this finer version of **ImpAs-Purolite**, and consequently a lower experimental error (with a more accurately measured arsenate capacity of  $40 \pm 2 \text{ mg g}^{-1}$ ). **ImpAs-Merrifield** similarly shows improved arsenate capacity ( $31 \pm 5 \text{ mg g}^{-1}$ ) compared to **ImpAs-HypoGel**. This is consistent with the number of active sites of the new polymer beads studied. In all cases, the  $Q_{\text{max}}$  calculated from the number of active sites is higher than the one obtained from the Langmuir isotherms, which could indicate that not all the active sites of the material are available for the removal of arsenate.

Table 2 Ligand and zinc(II) loading onto HypoGel and Purolite polymer beads, and compound **3** loading onto Merrifield polymer beads. The active sites of the three **ImpAs** sorbents, measured in triplicate, is also shown (see ESI† for calculations)

Polymer support	Ligand loading ( $\text{mmol g}^{-1}$ )	Zinc loading ( $\text{mmol g}^{-1}$ )	Compound <b>3</b> loading ( $\text{mmol g}^{-1}$ )	Active sites ( $\text{mmol g}^{-1}$ )
HypoGel	0.52	$0.53 \pm 0.01$	—	$0.27 \pm 0.01$
Purolite C106	0.68	$1.30 \pm 0.02$	—	$0.65 \pm 0.01$
Merrifield	—	—	0.22	$0.40 \pm 0.01$



**Table 3** Maximum removal capacity ( $Q_{\max}$ ) calculated using the number of active sites and the Langmuir model ( $Q_{\max}$ , affinity coefficient and  $R^2$ ). Experiments were carried out in triplicate

Sorbent	Active sites (mmol g <sup>-1</sup> )	Calculated $Q_{\max}$ (mg g <sup>-1</sup> )	Affinity coefficient $b$ (L mg <sup>-1</sup> )	Langmuir model, $Q_{\max}$ (mg g <sup>-1</sup> )	$R^2$
ImpAs-HypoGel	0.27 ± 0.01	37.36	3.0 ± 2.0	24 ± 3	0.9975
ImpAs-Purolite	0.65 ± 0.01	90.95	0.7 ± 0.5	36 ± 13	0.9403
Ground ImpAs-Purolite	0.65 ± 0.01	90.95	1.7 ± 0.7	40 ± 2	0.9935
ImpAs-Merrifield	0.40 ± 0.01	55.97	2.0 ± 1.0	31 ± 5	0.9554

### 3.3 Arsenate removal by flow-through experiments

Following the determination of the arsenate binding capacity of the different polymeric materials, we assessed their arsenate removal capacity in flow-through configuration. To this end, 1 g of the corresponding polymeric material was packed into 10 mL polypropylene columns between two filters, to prevent the leaching of the solid (Fig. 2). Two different aqueous solutions containing 15 µg L<sup>-1</sup> (which represents a concentration just above the WHO recommend upper limit) or 300 µg L<sup>-1</sup> (which represents high levels found in some areas in Bangladesh and India) of arsenate were passed through each of these columns using a peristaltic pump at two different flow rates (1 and 5 mL min<sup>-1</sup>). Fig. 5 shows that **ImpAs-Merrifield** has a similar arsenate removal ability in flow to **ImpAs-HypoGel**.

**ImpAs-Purolite**, however, displayed lower arsenate scavenging ability in flow compared to the other two polymeric materials. This was surprising considering that **ImpAs-Purolite** has the highest capacity of all materials as determined in the batch experiments (see Table 3). Considering that Purolite beads have the largest size of the solid supports under study (300–1600 µm) the functionalised beads were physically grounded to generate a finer material

that would be easier to load and pack in the column. This had the desired effect since the ground **ImpAs-Purolite** displayed practically the same arsenate-removal ability as the original **ImpAs-HypoGel** beads.

When treating aqueous solutions containing high levels of arsenate (*i.e.* 300 µg L<sup>-1</sup>) all the materials, except not-ground **ImpAs-Purolite**, were able to remove over 98% of the arsenate present at both flow rates studied (*i.e.* 1 and 5 mL min<sup>-1</sup>), with the treated/effluent water containing less than 10 µg L<sup>-1</sup> (see Table S8†). We were then interested to see the percentage removal when using waters containing 15 µg L<sup>-1</sup> of arsenate – *i.e.* just above the upper limit for arsenic in drinking water recommended by the WHO. All the polymeric materials under study were able to decrease the arsenate concentration below 6 µg L<sup>-1</sup> at a 5 mL min<sup>-1</sup> flow rate, with even lower levels (below 3 µg L<sup>-1</sup> of arsenate) achieved when using 1 mL min<sup>-1</sup> flow rate (*i.e.* increasing the contact time).

The above flow-through experiments were not designed to determine breakthrough curves and material lifetimes, and thus only 300 mL aqueous solutions of arsenate were used. Nevertheless, it is possible to estimate what volume of water could be potentially treated considering the capacity of each ImpAs sorbent material (see Table 3) and the percentage removal obtained from the flow experiments. For example, the

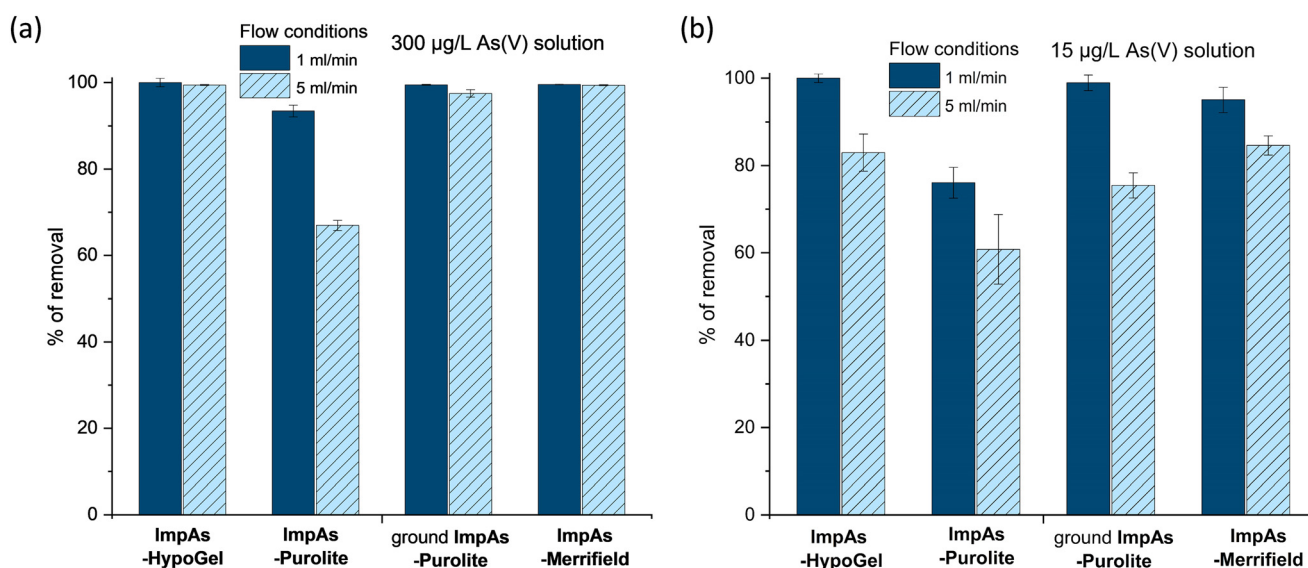


**Fig. 5** Percentage of arsenate removed by the different polymeric materials following flow through column experiments. Solutions with: (a) 300 µg L<sup>-1</sup> of arsenate and (b) 15 µg L<sup>-1</sup> of arsenate were treated at 1 mL min<sup>-1</sup> and 5 mL min<sup>-1</sup> flow rate.



capacity of ground **ImpAs-Purolite** is  $40 \text{ mg g}^{-1}$  (Table 3), and at a flow rate of  $1 \text{ mL min}^{-1}$ , it can remove 99% of the arsenate present in the flowing solution (for both the  $15$  and  $300 \text{ } \mu\text{g L}^{-1}$  arsenate solutions). Therefore, using  $1 \text{ g}$  of ground **ImpAs-Purolite** we would in principle be able to treat in flow *ca.*  $2000 \text{ L}$  of water containing  $20 \text{ } \mu\text{g L}^{-1}$  of arsenate (this level of arsenate is not uncommon in natural waters). For the other adsorbing materials herein studied, analogous calculations can be performed showing that they can treat between  $1200$  and  $1800 \text{ L}$  of water (see Table S10†). It should be noted that these values are estimates from water that contains arsenate but no other competing anions such as phosphate.

When selecting a material to remove pollutants from water, it is also important to consider the production costs. Since the four materials herein studied contain the same arsenate-binding receptor (*i.e.* compound **3** – see Fig. 1), the main cost differential of the sorbent material is the solid support. Based on the commercial providers we used, the approximate costs of HypoGel, Merrifield and Purolite C106 beads are  $\text{£}200$ ,  $\text{£}20$  and  $\text{£}1$  per  $100 \text{ g}$  of material respectively. The low cost of Purolite C106 and the excellent performance of ground **ImpAs-Purolite** makes this adsorbing material particularly suitable for removal of arsenate from large volumes of water.

## Conclusions

The main aim of the current study was to develop new functionalised polymer materials (based on our previously reported **ImpAs-HypoGel**) for the removal of arsenate from water. The two main drivers were to increase the arsenate removal capacity and reduce the cost of production. The data presented in this study shows that the di-zinc(II) receptor (**3**) can be attached onto different polymeric supports (*i.e.* HypoGel, Purolite C106 and Merrifield) to generate materials that remove arsenate from water to levels well below  $10 \text{ } \mu\text{g L}^{-1}$  (*i.e.* the upper limited of arsenic in drinking water recommended by the WHO). The commercial Purolite C106 polymer beads have five times higher capacity than HypoGel (based on  $\text{mmol}$  of COOH functional groups per gram of material) and therefore it can be functionalised with the arsenate receptor at a higher density. This has been confirmed by the batch studies which show that ground **ImpAs-Purolite** has a higher arsenate removal capacity ( $40 \text{ mg g}^{-1}$ ) than the original **ImpAs-HypoGel** ( $24 \text{ mg g}^{-1}$ ). The flow-through investigations have shown that ground **ImpAs-Purolite** can remove over 99% of arsenate present in solutions with both low ( $15 \text{ } \mu\text{g L}^{-1}$ ) and high ( $300 \text{ } \mu\text{g L}^{-1}$ ) levels of arsenate. While the degree of removal depends on the flow rate (with better performance at  $1 \text{ mL min}^{-1}$  than at  $5 \text{ mL min}^{-1}$ ), we show that even at the higher flow rate, ground **ImpAs-Purolite** reduces the levels of arsenate in the treated water to  $2.3$  and  $7.6 \text{ } \mu\text{g L}^{-1}$  for the two types of waters treated (*i.e.* low and high arsenate content respectively). Similar results were obtained with the other two polymeric materials herein presented. Furthermore, since Purolite C106 is  $200$  and  $20$  times cheaper than HypoGel and Merrifield

respectively, the cost of producing **ImpAs-Purolite** is significantly lower than the other two materials under study. This opens the possibility of producing **ImpAs-Purolite** at a significantly lower cost and with this, the possibility of scaling up for water treatment applications.

## Conflicts of interest

There are no conflicts to declare.

## Acknowledgements

We thank CONACYT for a fellowship to A. T. H. and the Engineering and Physical Sciences Research Council (EPSRC) Doctoral Training Centre in the Advanced Characterisation of Materials (CDT ACM) [grant number EP/L015277/1] for a studentship to J. C. B.

## References

- 1 S. H. Frisbie and E. J. Mitchell, *PLoS One*, 2022, **17**, e0263505.
- 2 P. Sen and T. Biswas, *Br. Med. J.*, 2013, **346**, f3625.
- 3 N. J. Raju, *Environ. Res.*, 2022, **203**, 111782.
- 4 J. G. Hering, I. A. Katsoyiannis, G. A. Theoduloz, M. Berg and S. J. Hug, *J. Environ. Eng.*, 2017, **143**, 03117002.
- 5 M. F. Naujokas, B. Anderson, H. Ahsan, H. V. Aposhian, J. H. Graziano, C. Thompson and W. A. Suk, *Environ. Health Perspect.*, 2013, **121**, 295–302.
- 6 L. Weerasundara, Y. S. Ok and J. Bundschuh, *Environ. Pollut.*, 2021, **268**, 115668.
- 7 K. Gupta, P. Joshi, R. Gusain and O. P. Khatri, *Coord. Chem. Rev.*, 2021, **445**, 214100.
- 8 L. L. Hao, M. Z. Liu, N. N. Wang and G. J. Li, *RSC Adv.*, 2018, **8**, 39545–39560.
- 9 A. D. Gupta, E. R. Rene, B. S. Giri, A. Pandey and H. Singh, *J. Environ. Chem. Eng.*, 2021, **9**, 106376.
- 10 B. An, Z. L. Fu, Z. Xiong, D. Y. Zhao and A. K. SenGupta, *React. Funct. Polym.*, 2010, **70**, 497–507.
- 11 B. An, T. R. Steinwinder and D. Y. Zhao, *Water Res.*, 2005, **39**, 4993–5004.
- 12 A. Dominguez-Ramos, K. Chavan, V. Garcia, G. Jimeno, J. Albo, K. V. Marathe, G. D. Yadav and A. Irabien, *Ind. Eng. Chem. Res.*, 2014, **53**, 18920–18927.
- 13 C. D. Moffat, D. J. Weiss, A. Shivalingam, A. J. P. White, P. Salaun and R. Vilar, *Chem. – Eur. J.*, 2014, **20**, 17168–17177.
- 14 S. Pal, T. K. Ghosh, R. Ghosh, S. Mondal and P. Ghosh, *Coord. Chem. Rev.*, 2020, **405**, 213128.
- 15 I. Ravikumar and P. Ghosh, *Chem. Soc. Rev.*, 2012, **41**, 3077–3098.
- 16 R. Dutta and P. Ghosh, *Chem. Commun.*, 2015, **51**, 9070–9084.
- 17 R. K. Egdal, G. Raber, A. D. Bond, M. Hussain, M. P. B. Espino, K. A. Francesconi and C. J. McKenzie, *Dalton Trans.*, 2009, 9718–9721.
- 18 S. K. Dey, B. Gil-Hernandez, V. V. Gobre, D. Woschko, S. S. Harmalkar, F. R. Gayen, B. Saha, R. L. Goswamee and C. Janiak, *Dalton Trans.*, 2022, **51**, 15239–15245.



- 19 S. I. Etkind, D. A. Vander Griend and T. M. Swager, *J. Org. Chem.*, 2020, **85**, 10050–10061.
- 20 J. C. Bullen, A. Torres-Huerta, P. Salaun, J. S. Watson, S. Majumdar, R. Vilar and D. J. Weiss, *Water Res.*, 2020, **175**, 115650.
- 21 Purolite®, Purolite C106. Product data sheet, 2019, Available at: <https://www.purolite.com/product/c106>.
- 22 HypoGel®, Product data available at: <https://www.rapp-polymer.com/index.php?id=220&currency=734>.
- 23 Merrifield Resin, Data available at: <https://www.sigmaaldrich.com/>.
- 24 A. J. Surman, C. S. Bonnet, M. P. Lowe, G. D. Kenny, J. D. Bell, E. Toth and R. Vilar, *Chem. – Eur. J.*, 2011, **17**, 223–230.
- 25 S. Svane, F. Kjeldsen, V. McKee and C. J. McKenzie, *Dalton Trans.*, 2015, **44**, 11877–11886.

